doi:10.1111/j.1558-5646.2007.00029.x

POLYGENIC TRAITS AND PARASITE LOCAL ADAPTATION

Benjamin J. Ridenhour[1,2] and Scott L. Nuismer[1]

[1] *Department of Biological Sciences, University of Idaho, Moscow, Idaho, 83844*

[2] *E-mail: bridenho@uidaho.edu*

Received June 6, 2006
Accepted October 21, 2006

The extent to which parasites are locally adapted to their hosts has important implications for human health and agriculture. A recently developed conceptual framework—the geographic mosaic theory of coevolution—predicts that local maladaptation should be common and largely determined by the interplay between gene flow and spatially variable reciprocal selection. Previous investigation of this theory has predominately focused on genetic systems of infection and resistance characterized by few genes of major effect and particular forms of epistasis. Here we extend existing theory by analyzing mathematical models of host–parasite interactions in which host resistance to parasites is mediated by quantitative traits with an additive polygenic basis. In contrast to previous theoretical studies predicated upon major gene mechanisms, we find that parasite local maladaptation is quite uncommon and restricted to one specific functional form of host resistance. Furthermore, our results show that local maladaptation should be rare or absent in studies that measure local adaptation using reciprocal transplant designs conducted in natural environments. Our results thus narrow the scope over which the predictions of the geographic mosaic theory are likely to hold and provide novel and readily testable predictions about when and where local maladaptation is expected.

KEY WORDS: **Antagonistic coevolution, gene flow, host-parasite, local adaptation, polygenic traits.**

Coevolution generates biological diversity, molds the ecological structure of communities, and drives tight coadaptation between species (e.g., Thompson 2005). However, an increasing number of empirical and theoretical studies suggests coevolution may lead to local maladaptation as well (Morand et al. 1996; Kaltz and Shykoff 1998; Kaltz et al. 1999; Thompson et al. 2002; Forde et al. 2004; Morgan et al. 2005). These observations have been incorporated as a key component of the geographic mosaic theory of coevolution, which predicts that moderate levels of local maladaptation should be a common consequence of the interplay between selection mosaics, coevolutionary hotspots, and gene flow, which characterizes interspecific interactions (Thompson 1994, 2005).

Theoretical studies have provided general support for the predictions of the geographic mosaic theory by demonstrating how gene flow and/or selection mosaics can interact to generate parasite local maladaptation (Gandon et al. 1996; Hochberg and van Baalen 1998; Nuismer et al. 1999; Thrall and Burdon 1999; Gandon 2002; Nuismer 2006). These results have, however, been derived by assuming host resistance to parasites is controlled by one or several loci of major effect and a particular form of epistasis—such as the epistasis present in inverse matching-alleles (Frank 1992), matching-alleles (Frank 1992), and gene-for-gene (Flor 1956; Parker 1994) models—rather than by quantitative traits with an additive polygenic basis. Nevertheless, quantitative traits mediate many naturally occurring antagonistic interactions, including host–parasite interactions (Berenbaum and Zangerl 1992; Bergelson et al. 2001; Zhong et al. 2003), and the majority of interactions between predators and prey (Brodie and Ridenhour 2002; Benkman et al. 2003; Dorner and Wagner 2003). However, no theoretical basis currently exists for evaluating the geographic mosaic theory in these biologically diverse and important cases. In addition to these genetic assumptions, previous studies have generally assumed that local adaptation is measured in a homogenous laboratory environment (Nuismer 2006) rather than in the field, and thus capture only one or a few components of local adaptation.

© 2007 The Author(s)
Journal compilation © 2007 The Society for the Study of Evolution

To fill this gap, we use two complementary approaches to understanding the evolutionary dynamics of local adaptation in antagonistic interactions controlled by polygenic traits: (1) Analytical quantitative genetic models are used to find solutions under conditions of weak selection and fixed genetic variance, and (2) deterministic numerical simulations explore situations with strong selection and evolving genetic variances. We analyze cases in which phenotype matching or phenotype escalation mediates resistance to infection. Finally, the effect of experimental design on measures of local adaptation is considered.

Methods

ANALYTICAL MODEL

We develop a mathematical model of spatially structured host–parasite coevolution mediated by quantitative traits. We assume both host and parasite are distributed across two discrete habitat patches connected by host (m_H) and parasite (m_P) gene flow and assume that population sizes are large enough for the effects of genetic drift to be negligible. Species encounters occur randomly within patches, with the probability of successful parasite infection determined by quantitative traits in the host (z_H) and the parasite (z_P).

Our model incorporates two common functional forms of resistance: phenotype matching and phenotype escalation. The phenotype-matching model assumes that host resistance increases as the phenotypes of the interacting individuals become increasingly dissimilar (Dieckmann et al. 1995; Gavrilets 1997; Abrams 2000; Soler et al. 2001) (Fig. 1A). In contrast, the phenotype escalation model assumes that host resistance increases with host phenotype (Berenbaum and Zangerl 1992; Gavrilets 1997; Brodie et al. 2002) (Fig. 1B). In both cases, we assume that infection reduces host fitness by an amount (s_H) and that resistance reduces parasite fitness by an amount (s_P) within the native environment; we use T_H and T_P to denote fitness consequences in the environment in which local maladaptation is measured (e.g., laboratory, common garden, field). Finally, our model incorporates spatially homogenous Gaussian stabilizing selection.

Our general model can be used to predict the level of local adaptation for either functional form of host resistance if selection is assumed to be weak. Because some studies of local adaptation employ reciprocal cross-infection designs (RCI) whereas others use reciprocal transplant (RT) designs, we calculate local adaptation for each. RCI studies generally measure local adaptation in the *laboratory* as the difference in average *infection* frequency of parasites challenged with sympatric and allopatric hosts and hosts challenged with sympatric and allopatric parasites (Altizer 2001; Jokela et al. 2003; Lively et al. 2004). In contrast, RT designs generally measure local adaptation in the *field* as the difference in average *fitness* between individuals raised in their native environment and individuals raised in a foreign environment (Angert and Schemske 2005; Griffith and Watson 2005).

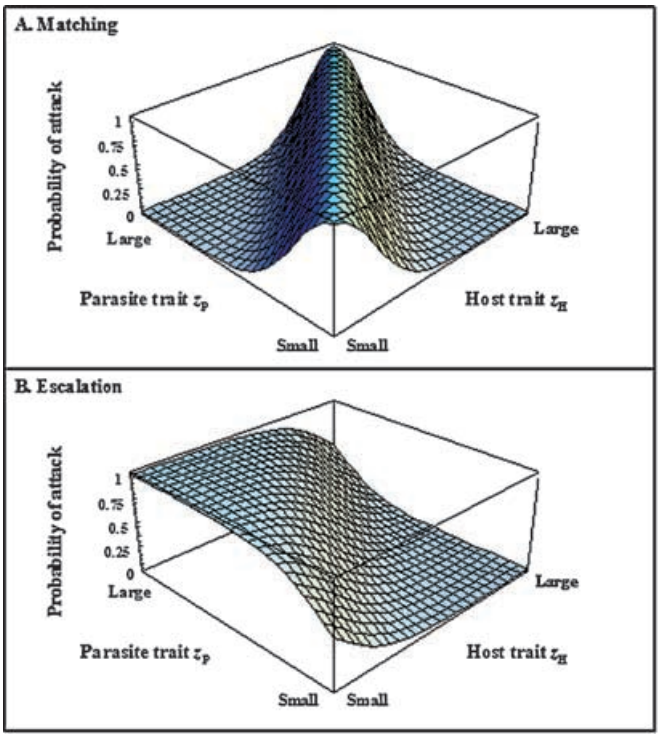

Figure 1. Probability of infection surfaces based on phenotype matching or phenotype escalation. Each surface depicts how the probability of successful infection by a parasite shifts with changes in host and parasite phenotypes. Panel A shows the relationship between parasite (z_P) and host (z_H) phenotypes and the probability of infection for the phenotype matching model; Panel B shows the same relationship for the phenotype escalation model.

We calculate the local adaptation for either species (Λ_i) based upon the fitness functions for phenotype matching and phenotype escalation. Following standard conventions, local adaptation is defined as

$$\Lambda_i = (\bar{W}_{i,1,1} - \bar{W}_{i,1,2} + \bar{W}_{i,2,2} - \bar{W}_{i,2,1})/2 \qquad (1)$$

where the bar notation indicates the expectation of a variable (population mean fitness in this case) and the subscripts indicate species, population of origin for the host or parasite, and test environment, respectively. The test environment typically is the population of parasite or host, respectively, to be tested in or against. This mathematical definition of local adaptation is consistent with both the home versus away and local versus foreign concepts of local adaptation for the case of two patches considered here (cf. Kawecki and Ebert 2004 for a discussion of these measures).

For either phenotype matching or escalation, we define fitness as

$$W_H = e^{-\gamma_H(z_H-\theta_H)^2} \times [1 - s_H P(z_H, z_P)] \qquad (2a)$$

for the host and

$$W_P = e^{-\gamma_P(z_P-\theta_P)^2} \times [1 - s_P(1 - P(z_H, z_P))] \quad (2b)$$

for the parasite. In equation (2), the parameter γ_i controls the strength of stabilizing selection in species i toward an optimum phenotypic value (θ_i). As mentioned before, we assume γ_i and θ_i are spatially homogenous, as would be the case if resistance and infectivity impose a fitness cost that is constant across environments.

The probability of successful infection ($P(z_H,z_P)$) is defined differently for the phenotype matching and the phenotype escalation models. For phenotype matching the probability of a successful infection is defined as

$$P(z_H, z_P) = e^{-\alpha(z_H-z_P)^2}, \quad (3a)$$

whereas the same probability under the phenotype escalation model is

$$P(z_H, z_P) = 1/\left(1 + e^{\alpha(z_H-z_P)}\right). \quad (3b)$$

The parameter α determines the sensitivity of the probability of successful infection to changes in host and parasite phenotypes. In all cases, we assume that α is spatially homogenous. We use a Taylor series (see Supporting Information) of our fitness functions to approximate the population mean fitness values in (1). Taylor series approximation was necessitated by the fact that population mean fitness cannot be calculated exactly for our fitness functions.

To model the evolution of polygenic traits, we use the quantitative genetic framework developed by Lande (1979) and Lande and Arnold (1983). Thus, we calculate the evolutionary change in the mean phenotype ($\Delta\bar{z}_i$) due to selection as

$$\Delta\bar{z}_i = G_i \frac{\partial \ln \bar{W}_i}{\partial \bar{z}_i}, \quad (4)$$

where G_i is the genetic variance of the trait. The average phenotype after selection ($\bar{z}_i'$) is

$$\bar{z}_i' = \Delta\bar{z}_i + \bar{z}_i \quad (5a)$$

which, with migration (m_i) between populations j and k taken into account, becomes

$$\bar{z}_{i,j}'' = (1 - m)(\Delta\bar{z}_{i,j} + \bar{z}_{i,j}) + m_i(\Delta\bar{z}_{i,k} + \bar{z}_{i,k}). \quad (5b)$$

The variable $\bar{z}_{i,j}''$ is the mean phenotype in population j after a bout of selection and migration.

DETERMINISTIC NUMERICAL SIMULATIONS

We used deterministic numerical simulations to extend our analysis to cases in which selection is strong and genetic variances evolve. These simulations assume that host and parasite phenotypes are determined by the additive action of between one and five haploid, diallelic loci. Specifically, an individual's phenotype (z_i) was calculated as

$$z_i = \sum_{j=1}^{n} X_j/n \quad (6)$$

where X_j takes a value of 1 if the individual carries a "1" allele at locus j, but a value of 0 if an individual carries a "0" allele at locus j; n is the number of loci. Consequently, z_i was bounded on the interval [0,1]. In addition, we assumed that all loci recombined freely and underwent mutation between allelic states at a rate of 1×10^{-6} per locus.

Simulations used the same functions as the analytical models for selection due to species interactions and the abiotic environment (eq. 2); gene flow, too, was incorporated into simulations in the same way as in the analytical models (eq. 5b). For both matching and escalation models, we ran extensive simulations spanning a wide range of fitness consequences and rates of gene flow. In each case, we calculated the average local maladaptation for host and parasite using both RT and RCI designs.

Each simulation run began with allele frequencies selected at random from a uniform distribution. Parameter values were randomly drawn from uniform distributions over the following intervals: $\alpha\in[1,4]$, $\bar{s}_i \in [0.05, 05]$, $\delta_{s,i}\in[-2\bar{s}_i,2\bar{s}_i]$, $m_i\in[0,0.1]$, $\theta_i\in[0,1]$, and $\gamma_i \in[0,2.5]$ where $\bar{s}_i = (s_{i,1} + s_{i,2})/2$ and $\delta_{s,i} = s_{i,1} - s_{i,2}$. By necessity, the parameter ranges are somewhat arbitrary, and were chosen based upon the following considerations. The range of strengths of stabilizing selection (γ_i) was constrained so as not to overwhelm coevolutionary selection. Rates of gene flow (m_i) were kept relatively small to prevent the genetic homogenization of the populations and the inevitable loss of all local adaptation or maladaptation. The average strength of coevolutionary selection ranged from weak ($\bar{s}_i = 0.05$) to very strong ($\bar{s}_i = 0.5$), and the range of $\delta_{s,i}$ was chosen to allow levels of spatial variation to vary from completely homogenous to strongly heterogeneous (in which case one population was a coevolutionary hotspot and the other was a coevolutionary coldspot). Values of α were constrained to lie between one and four, representing cases ranging from a probability of infection that varied only weakly with the phenotypes of the interacting species ($\alpha = 1$) to cases in which slight changes in host and parasite phenotype had large consequences for the probability of infection ($\alpha = 4$).

The average value of local adaptation was calculated for each species over the final 2000 simulation generations (i.e., generations 2000–4000) using the same formulae as the analytical model (eq. 1). Local adaptation values were averaged across the final 2000 generations to represent the expected level of local adaptation even in those cases in which cyclical dynamics occurred (Gandon 2002). Our simulations resulted in a preponderance of zero values for local adaptation (Fig. 2); this large number of

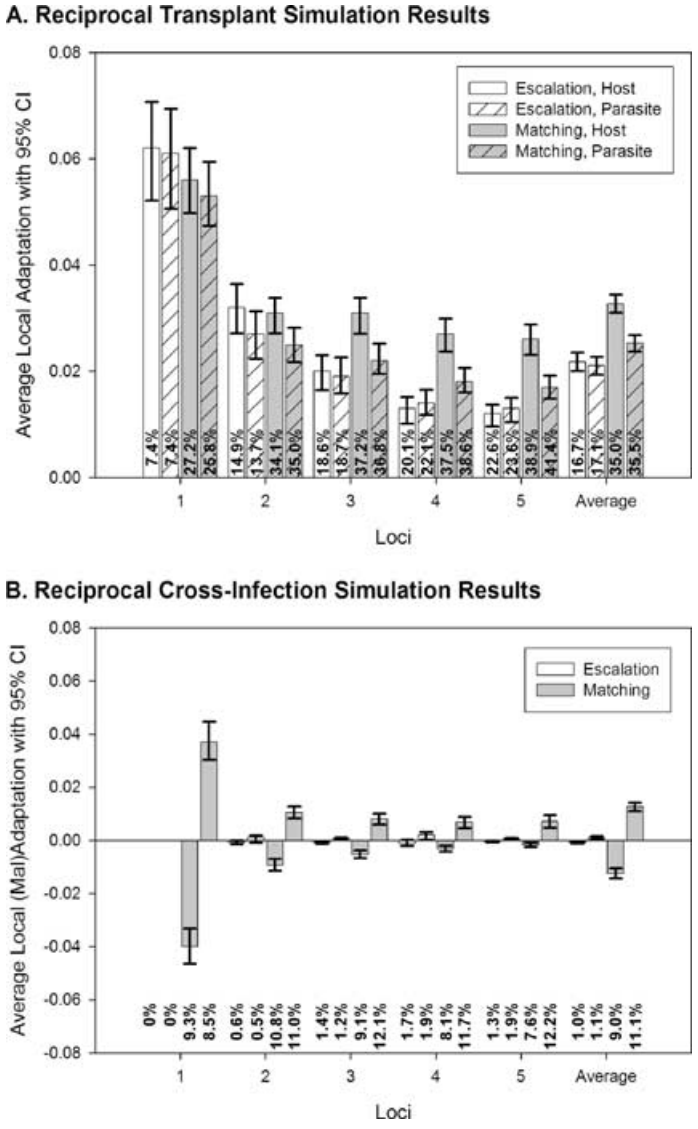

Figure 2. **Average values of local (mal)adaptation based on simulations broken down by loci. Panel A shows local adaptation as would be measured in reciprocal transplant experiments. Local maladaptation results are not given because only 7 and 5 of 20,000 simulations resulted in local maladaptation for the host and parasite, respectively. Panel B shows both local maladaptation and local adaptation results for parasites if experiments were done as reciprocal cross-infections. For each locus there are four bars that respectively (left to right) correspond to: mean parasite local maladaptation in the escalation model, mean parasite local adaptation in the escalation model, mean parasite local maladaptation in the matching model, and mean parasite local adaptation in the matching model. Host results are not shown because they are equal in magnitude but opposite in sign to the parasite results. Percentages along the x-axis in both A and B indicate how often a particular result was observed (e.g., for a trait controlled by four loci, 1.7% of cases resulted in parasite local maladaptation when using an RCI experiment). The error bars indicate the 95% confidence interval for the mean.**

zeroes essentially guarantees nonsignificant effects of all parameters on the magnitude of local adaptation if standard linear regression analysis was used. However, by using ordinal logistic regression on a discrete version of local adaptation, we can test whether a parameter affects the probability of being either locally maladapted, zero, or locally adapted. Thus, for our ordinal logistic analysis, local adaptation was used as our response variable and was coded as (0) if the value was negative indicating local maladaptation, (1) if the value was approximately zero (within $\pm 1 \times 10^{-5}$), indicating an absence of both local adaptation and local maladaptation, or (2) if the value was positive indicating local adaptation. All model parameters as well as number of loci were included in the analysis as explanatory variables. In addition to estimating the effects of linear combinations of parameters, we included the product $\delta_{s,\mathrm{H}} \times \delta_{s,\mathrm{P}}$ as an explanatory variable because of its importance in previous models of local adaptation (Nuismer 2006) and because analytical results reported below suggested a role for the interaction between these parameters. We used R (R. Development Core Team 2006) to perform all statistical analyses.

Results

ANALYTICAL MODEL RESULTS

Our analysis reveals that the magnitude and sign of local adaptation depends heavily on both the functional form of host resistance and on the experimental design used to measure local adaptation. Specifically, we find that when host resistance follows the escalation model, local adaptation (Λ_i^{E}) measured for a species (i) is

$$\Lambda_i^{\mathrm{E}} = \frac{1}{8}\alpha(T_{i,1} - T_{i,2})(\bar{z}_{i,1} - \bar{z}_{i,2}) \qquad (7)$$

where $T_{i,j}$ is the fitness consequence of interactions in species i and test environment j. Equation (7) shows that the measured level of local adaptation depends upon the sensitivity of host resistance to host and parasite phenotypes (α, see Fig. 1), the fitness consequences of the interaction within the test environment(s), and the trait means in the two populations. In an RCI experiment, local adaptation is estimated based upon studies conducted in a homogenous laboratory environment, and thus the fitness consequences of interactions are also homogenous ($T_{i,1} = T_{i,2}$). Thus, equation (7) shows that for RCI studies, local adaptation will be zero for systems mediated by phenotype escalation. In contrast, for RT experiments the test environments are the native environments. The fitness consequences of interacting are therefore those of the native environment ($T_{i,j} = s_{i,j}$). In contrast to RCI experiments, RT experiments generally lead to nonzero levels of local adaptation (as long as $s_{i,1} \neq s_{i,2}$) for the model of phenotype escalation.

Unlike phenotype escalation, local adaptation is possible in the matching model for both RCI and RT designs. Specifically, local adaptation (Λ_i^{M}) for phenotype matching is

$$\Lambda_i^{\mathrm{M}} = \alpha(\bar{z}_{i,1} - \bar{z}_{i,2})[(\bar{\bar{z}}_{\mathrm{H}} - \bar{\bar{z}}_{\mathrm{P}})(T_{i,1} - T_{i,2}) + \frac{\omega_i}{2}(\bar{z}_{i',1} - \bar{z}_{i',2})(T_{i,1} + T_{i,2})], \quad (8)$$

where $\omega_{\mathrm{P}} = 1$ and $\omega_{\mathrm{H}} = -1$. Equation (8) differs from equation (7) in several respects, the most critical being an additional term not multiplied by zero if $T_{i,1} = T_{i,2}$. The important consequence of this additional term is that local adaptation need not be zero in an RCI experiment. Equation (8) also differs from (7) by depending on the trait means of the opposing species ($\bar{z}_{i',j}$) and the phenotypic average across both patches ($\bar{\bar{z}}_i$).

Although our results for local adaptation (eqs. 7 and 8) are quite general, they depend upon the trait means of both host and parasite. Therefore, we formulated approximate quasi-equilibrium solutions for the host and parasite trait means and evaluated our definitions at these points (see Supporting Information). As previously stated, our approach uses a standard quantitative genetics framework that assumes weak selection and fixed genetic variance (G_i) (Lande 1979; Lande and Arnold 1983). In addition, to make our model analytically tractable, we assume that stabilizing selection is weak relative to coevolutionary selection and, in the matching model, that the rate of gene flow is large relative to spatial variability in selection (Nagylaki 1980; Whitlock and Gomulkiewicz 2005).

The resulting expressions for the spatial difference in mean phenotypes demonstrate important roles for gene flow and spatial differences in fitness consequences of interactions (i.e., selection mosaics; see Supporting Information). For phenotype escalation, we find the difference in mean phenotypes between populations is given by

$$(\bar{z}_{i,1} - \bar{z}_{i,2}) = \frac{1}{8} \times \frac{\alpha G_i(1 - 2m_i)(s_{i,1} - s_{i,2})}{\gamma_i G_i(1 - 2m_i) + m_i}. \quad (9)$$

When phenotype matching governs coevolution, the analogous quantity is

$$(\bar{z}_{i,1} - \bar{z}_{i,2}) = \frac{\alpha G_i(1 - 2m_i)(\bar{\bar{z}}_{\mathrm{H}} - \bar{\bar{z}}_{\mathrm{P}})(s_{i,1} - s_{i,2})}{m_i}. \quad (10)$$

Equations (9) and (10) yield two important insights: First, no difference in mean phenotypes exists if there are no spatial differences in fitness consequences (i.e., no selection mosaics). Second, gene flow acts strictly as a homogenizing force for both escalatory and matching systems ($\partial|(\bar{z}_{i,1} - \bar{z}_{i,2})|/\partial m_i < 0$); as gene flow increases, the difference in mean phenotypes decreases.

Equations (7–10) allow us to derive explicit expressions for the sign and magnitude of local adaptation at any point in time (see Supporting Information). We find several important and unexpected results. First, for RT studies, escalation *always* leads to local adaptation in both host and parasite. Thus, phenotype escalation never produces local maladaptation irrespective of experimental design. Second, in matching systems local adaptation should be much more common in RT than RCI studies (see Supporting Information). Third, the product of the parasite and host selection mosaics ($(s_{\mathrm{P},1} - s_{\mathrm{P},2}) \times (s_{\mathrm{H},1} - s_{\mathrm{H},2})$ or equivalently $\delta_{s,\mathrm{P}} \times \delta_{s,\mathrm{H}}$) may be used as as predictor for local adaptation in systems mediated by phenotype matching (see Supporting Information). Finally, increased rates of host gene flow reduce the magnitude of host local adaptation (see Supporting Information) regardless of the rate of gene flow in the parasite, and vice versa.

SIMULATION RESULTS

Simulations conducted under conditions of strong selection and evolving genetic variances provided broad support for our key analytical predictions. The raw data from these simulations are available in the form of Microsoft™ Excel files upon request. The simulations demonstrate that parasite local maladaptation is practically absent from RT experiments with 0% and 0.05% of cases showing local maladaptation for phenotype escalation and matching, respectively (Fig. 2A). In contrast, local maladaptation occurred in approximately 9% and 11% of all cases for the parasite and host, respectively in RCI experiments for the phenotype-matching model (Fig. 2B). For the escalation model, local maladaptation is very rare if an RCI design is used (∼1% of all cases for the host and parasite; Fig. 2B), and the average value of local adaptation is approximately zero as predicted (Fig. 2B).

The number of loci controlling the host and parasite traits also affected the frequency and magnitude of local adaptation. The effect of loci on the probability of being locally adapted was significant in all ordinal logistic regression models (Tables 1 and 2) except for the phenotype escalation-RCI model that was not significant overall (Table 1). The phenotype escalation-RCI was not significant because very few cases with either local maladaptation or adaptation existed (∼2%). Furthermore, in RT experimental designs this effect was significantly nonlinear (Tables 1 and 2). In addition to affecting the frequency of local adaptation, the number of loci nonlinearly affected the magnitude of local (mal)adaptation for both phenotype matching (RCI and RT; Fig. 2) and escalation (RT only; Fig. 2).

Our ordinal logistic regression also yielded insight into the impact of other model parameters. We see that, as predicted, the product of the selection mosaic ($\delta_{s,\mathrm{P}} \times \delta_{s,\mathrm{H}}$) has a significant effect on the probability of local adaptation in phenotype matching but not in phenotype escalation (Tables 1 and 2). The effect of this product on the probability of being locally adapted differs between RCI and RT designs however. For RCI experiments,

Table 1. Results of ordinal logistic regression analysis for the model of phenotype escalation. Positive parameter estimates indicate factors that increase the probability of being locally adapted as the parameter value increases. Host RCI results are not shown because they are exactly equal in magnitude to the parasite RCI results but opposite in sign.

Effect	Parasite, RT	Host, RT	Parasite, RCI
Loci	0.8275[d]	0.9322[d]	−0.0202
Nonlinear	NA[d]	NA[d]	NA
θ_H	0.3596[c]	−1.8015[d]	−0.0174
γ_H	−0.1116[b]	−0.4506[d]	−0.0148
θ_P	−1.9612[d]	0.6203[d]	0.3154
γ_P	−0.5641[d]	−0.1348[c]	−0.0315
α	0.3010[d]	0.2729[d]	0.0002
$\bar{s}_H$	0.4779[a]	5.2112[d]	0.0305
$\delta_{s,H}$	0.0926	0.1134	−0.2728
$\bar{s}_P$	5.4136[d]	0.5906[b]	0.6279
$\delta_{s,P}$	0.1206	−0.0155	0.1884
$\delta_{s,P} \times \delta_{s,H}$	0.0956	−0.1055	1.1488[a]
m_H	−0.7201	−20.6174[d]	−2.5028
m_P	−22.5343[d]	0.7972	0.3966
Model	NA[d]	NA[d]	NA

[a]$P<0.05$, [b]$P<0.01$, [c]$P<0.001$, [d]$P<0.0001$.

Table 2. Results of ordinal logistic regression analysis for the model of phenotype matching. Positive parameter estimates indicate factors that increase the probability of being locally adapted as the parameter value increases. Host RCI results are not shown because they are exactly equal in magnitude to the parasite RCI results but opposite in sign.

Effect	Parasite, RT	Host, RT	Parasite, RCI
Loci	0.5496[d]	0.4149[d]	0.0683
Nonlinear	NA[d]	NA	NA
θ_H	−0.0123	0.0096	−0.0991
γ_H	−0.3748[d]	−0.243[d]	0.0608
θ_P	0.1783[a]	−0.0037	0.0247
γ_P	−0.7950[d]	−0.5691[d]	−0.2140[d]
α	0.4006[d]	0.2561[d]	0.0187
$\bar{s}_H$	2.4100[d]	4.7509[d]	0.9991[d]
$\delta_{s,H}$	0.0637	0.1203[a]	−0.0365
$\bar{s}_P$	5.0968[d]	1.7940[d]	0.1422
$\delta_{s,P}$	−0.0972	−0.1565[b]	−0.0017
$\delta_{s,P} \times \delta_{s,H}$	0.5549[b]	0.4589[b]	2.4531[d]
m_H	0.4256	−9.5725[d]	−5.3912[d]
m_P	−14.1586[d]	−1.7920	2.1448[a]
Model	NA[d]	NA[d]	NA[d]

[a]$P<0.05$, [b]$P<0.01$, [c]$P<0.001$, [d]$P<0.0001$.

as in Nuismer (2006), if $\delta_{s,P} \times \delta_{s,H} > 0$ we expect the probability of the parasite being locally adapted to increase and the probability of the host being locally *maladapted* to increase as the magnitude of the product of the selection mosaic increases (Table 2). In contrast, if $\delta_{s,P} \times \delta_{s,H} > 0$, we increasingly expect *both* host and parasite to be locally *adapted* in RT experiments as the magnitude of the product increases. We also see that, with the exception of RCI experiments involving interactions mediated by phenotype matching, the rate of gene flow in the interacting species does not affect local adaptation (Tables 1 and 2).

Discussion

Our analytical and numerical results suggest that local maladaptation—a key prediction of the geographic mosaic theory—is less prevalent for species interactions mediated by quantitative traits than those mediated by major gene mechanisms. This difference is particularly striking for cases in which host resistance is based on a model of phenotype escalation, as is likely the case for many interactions between plants and their insect parasites and predators and prey (Ehrlich and Raven 1964; Chew and Courtney 1991; Berenbaum and Zangerl 1992; Farrell and Mitter 1998). Moreover, our results demonstrate local maladaptation is less likely to be inferred when reciprocal transplant (RT) designs are used than when reciprocal cross infection (RCI) designs are used.

Specifically, in the phenotype escalation model, our simulations show that only local adaptation is possible for RT experiments and that RCI experiments yield almost entirely local adaptation values of zero (approximately 2% nonzero; Fig. 2B); both results were predicted by our analytical model. For the phenotype matching model, RT experiments again result in detecting local adaptation almost all of the time (only 5 of 10,000 cases yielded maladaptation), but RCI experiments do result in local maladaptation in approximately 10% of all cases (Fig. 2B). These results are in keeping with our analytical predictions as well.

In addition to showing that local maladaptation is generally less common for interactions mediated by polygenic traits, our results demonstrate the effect of experimental design on detecting local maladaptation (kingsolver and Gomulkiewicz 2003; Fuller et al. 2005). Specifically, our results show RCI can potentially yield local maladaptation whereas RTs do not (Fig. 2). Intuitively, our results can be best understood by considering the difference in the quantities local adaptation actually measures in reciprocal cross-infection versus RT studies. In general, RCI studies remove an organism from the natural fitness environment in which it evolved and measure only particular fitness components (e.g., the probability of infection). In contrast, in an RT study, local adaptation is measured in the environment in which the organism evolved

and measures all fitness components. This difference in context is the primary driver of the increased levels of local adaptation we observe in RT versus RCI experiments. For local maladaptation to occur, individuals must have a higher fitness score, on average, in their nonnative environment than in their native environment. In an RT experiment, this is unlikely, because the organism adapts according to all the fitness components and trade-offs of its natural environment. Consequently, we expect organisms to be closer, on average, to the fitness optimum of their native environment than to the fitness optimum of their nonnative environment. In contrast, in an RCI experiment, only a single component of fitness is measured in the absence of natural trade-offs. Because such trade-offs between fitness components play an integral part in the true fitness, organisms may be closer, on average, to the fitness optimum of their nonnative environment for traits measured in the laboratory. We hypothesize that this result arises because RCI designs measure only one component of fitness—the probability of successful infection/resistance; constraints caused by the abiotic environment or by spatial variation in fitness consequences of interactions are generally ignored in these designs.

In addition to confirming several of our analytical predictions, our simulations revealed interesting effects of increasing numbers of loci. As the number of loci increased, the frequency of local adaptation increased, but the magnitude of local adaptation decreased (Tables 1 and 2; Fig. 2). There was significant nonlinearity to this observation (Tables 1 and 2). Specifically, both the frequency of local adaptation and magnitude of local adaptation rapidly seemed to approach asymptotic values (Fig. 2). The apparent asymptotic behavior of local adaptation as a function of the number of loci suggests that our five locus simulations may yield a reasonable approximation for even larger numbers of loci, and thus may be a good approximation of our Gaussian analytical model. In contrast, when there are only very few loci, our simulation results may perhaps be better compared with previous major gene theory. For instance, it can be shown that the one locus version of the phenotype-matching model converges on a matching-alleles model, and the one locus version of the phenotype escalation model is similar to, but not the same as, a gene-for-gene model (see Supporting Information). Thus it is not entirely surprising that our one-locus phenotype-matching simulations under RCI conditions yield results similar to past major-gene models (e.g., Nuismer 2006).

Together, our results provide predictions that can be readily tested empirically. For instance, our prediction that local maladaptation should be significantly less common when measured using an RT design provides a particularly straightforward opportunity for empirical testing. Unfortunately, RT studies are relatively rare, particularly within the framework of host–parasite interactions, and thus meta-analysis comparing the results of these two methods is not currently feasible. Future empirical studies that measure parasite local adaptation using both RCI and RT designs would prove very valuable for testing this prediction. Similarly, our models predict that local maladaptation should not occur in those interactions mediated by phenotype escalation. To evaluate this prediction, studies of local adaptation need to be performed once it has been established that a particular interaction follows a model of phenotypic escalation. Logical candidates include interactions between camellia and their weevils (Toju and Sota 2006), parsnips and parsnip webworms (Berenbaum and Zangerl 1992), and newts and garter snakes (Brodie et al. 2002).

Our results also have implications for the results of empirical studies of parasite local adaptation that attribute observed levels of local adaptation to differences in the gene flow rates of the interacting species (Kaltz et al. 1999; Oppliger et al. 1999; McCoy et al. 2005; Prugnolle et al. 2005). Although the theoretical basis upon which the interpretation of these studies is quite robust when interactions are mediated by major gene mechanisms of resistance and local adaptation is measured using an RCI design (Gandon et al. 1996; Gandon 2002), our results show that this is not the case for polygenic traits or RT designs. We only observed relative gene flow rates affecting local adaptation for cross-infection studies of phenotype matching (Table 2). Consequently, it is important to have at least a rudimentary understanding of the genetic basis of the traits mediating an interaction, and the functional relationship between these traits and resistance, prior to attributing observed patterns of local adaptation to differences in the relative rates of host and parasite gene flow.

Our results also demonstrated a significant effect of the product of the selection mosaics on local adaptation in a phenotype-matching model (Table 2). Nuismer (2006) also found that this product was important to determining local adaptation in (inverse) matching-alleles models and gene-for-gene models. Our results indicate that this relationship is not universally true for polygenic traits, but may apply if the model of fitness for the polygenic trait converges on a major-gene model (as was the case for our phenotype matching model). Interestingly, we found that the effect of the product of the selection mosaic was different for RCI and RT experiments. Measuring local adaptation using RCI experiments yielded the same results as Nuismer (2006) in which the sign ($\pm$) of the selection mosaic determines whether the host or parasite is locally adapted. In contrast, our RT simulation results indicate that increases in the product of the selection mosaic favor local adaptation for both host and parasite (Table 2). These conflicting results seem to suggest that the product of the selection mosaics has different consequences for the probability of successful infection (measured using RCI) and overall organismal fitness (measured using RT).

Though we frame our results within host–parasite systems, our results may apply more broadly to other antagonistic interactions mediated by phenotype matching or escalation mechanisms. For instance, many interactions between predators and prey are apparently mediated by quantitative traits (Brodie et al. 2002; Benkman et al. 2003; Cook 2003; Dietl 2003; Dorner and Wagner 2003), and some of these appear to be matching (Cook 2003; Dorner and Wagner 2003) and others escalation (Brodie et al. 2002; Benkman et al. 2003; Dietl 2003). Similarly, many interactions between herbivorous insects and their food-plants may be mediated by quantitative traits and escalation. At the same time, however, the generality of our results may be constrained by our genetic and demographic assumptions. Addressing the impact of these assumptions issues should be an important focus of future work.

ACKNOWLEDGMENTS

We would like to thank the Palouse Coevolution Reading Group, J. Kelly, S. Gandon, and R. Mauricio for their helpful comments and suggestions on previous versions of this article. This research was funded by the NSF grants DEB 0343023 and DMS 0540392 to SLN.

LITERATURE CITED

Abrams, P. A. 2000. The evolution of predator-prey interactions: theory and evidence. Annu. Rev. Ecol. Syst. 31:79–105.

Altizer, S. M. 2001. Migratory behaviour and host-parasite co-evolution in natural populations of monarch butterflies infected with a protozoan parasite. Evol. Ecol. Res. 3:611–632.

Angert, A. L., and D. W. Schemske. 2005. The evolution of species' distributions: reciprocal transplants across the elevation ranges of *Mimulus cardinalis* and *M. lewisii*. Evolution 59:1671–1684.

Benkman, C. W., T. L. Parchman, A. Favis, and A. M. Siepielski. 2003. Reciprocal selection causes a coevolutionary arms race between crossbills and lodgepole pine. Am. Nat. 162:182–194.

Berenbaum, M. R., and A. R. Zangerl. 1992. Genetics of physiological and behavioral resistance to host furanocoumarins in the parsnip webworm. Evolution 46:1373–1384.

Bergelson, J., G. Dwyer, and J. J. Emerson. 2001. Models and data on plant-enemy coevolution. Annu. Rev. Genet. 35:469–499.

Brodie, E. D., and B. J. Ridenhour. 2003. Reciprocal selection at the phenotypic interface of coevolution. Integr. Comp. Biol. 43:408–418.

Brodie, E. D., B. J. Ridenhour, and E. D. Brodie. 2002. The evolutionary response of predators to dangerous prey: hotspots and coldspots in the geographic mosaic of coevolution between garter snakes and newts. Evolution 56:2067–2082.

Chew, F. S., and S. P. Courtney. 1991. Plant apparency and evolutionary escape from insect herbivory. Am. Nat. 138:729–750.

Cook, L. M. 2003. The rise and fall of the Carbonaria form of the peppered moth. Q. Rev. Biol. 78:399–417.

Dieckmann, U., P. Marrow, and R. Law. 1995. Evolutionary cycling in predator-prey interactions: population dynamics and the red queen. J. Theor. Biol. 176:91–102.

Dietl, G. R. 2003. Coevolution of a marine gastropod predator and its dangerous bivalve prey. Biol. J. Linn. Soc. 80:409–436.

Dorner, H., and A. Wagner. 2003. Size-dependent predator-prey relationships between perch and their fish prey. J. Fish Biol. 62:1021–1032.

Ehrlich, P. R., and P. H. Raven. 1964. Butterflies and plants: a study in coevolution. Evolution 18:586–608.

Farrell, B. D., and C. Mitter. 1998. The timing of insect/plant diversification: might Tetraopes (Coleoptera: Cerambycidae) and Asclepias (Asclepiadaceae) have co-evolved? Biol. J. Linn. Soc. 63:553–577.

Flor, H. H. 1956. The complementary genetic systems in flax and flax rust. Adv. Genet. 8:29–54.

Forde, S. E., J. N. Thompson, and B. J. M. Bohannan. 2004. Adaptation varies through space and time in a coevolving host-parasitoid interaction. Nature 431:841–844.

Frank, S. A. 1992. Models of plant pathogen coevolution. Trends Genet. 8:213–219.

Fuller, R. C., C. F. Baer, and J. Travis. 2005. How and when selection experiments might actually be useful. Integr. Comp. Biol. 45:391–404.

Gandon, S. 2002. Local adaptation and the geometry of host-parasite coevolution. Ecol. Lett. 5:246–256.

Gandon, S., Y. Capowiez, Y. Dubois, Y. Michalakis, and I. Olivieri. 1996. Local adaptation and gene-for-gene coevolution in a metapopulation model. Proc. R. Soc. Lond. Ser. B, Biol. Sci. 263:1003–1009.

Gavrilets, S. 1997. Coevolutionary chase in exploiter-victim systems with polygenic characters. J. Theor. Biol. 186:527–534.

Griffith, T. M., and M. A. Watson. 2005. Stress avoidance in a common annual: reproductive timing is important for local adaptation and geographic distribution. J. Evol. Biol. 18:1601–1612.

Hochberg, M. E., and M. van Baalen. 1998. Antagonistic coevolution over productivity gradients. Am. Nat. 152:620–634.

Jokela, J., C. M. Lively, M. F. Dybdahl, and J. A. Fox. 2003. Genetic variation in sexual and clonal lineages of a freshwater snail. Biol. J. Linn. Soc. 79:165–181.

Kaltz, O., and J. A. Shykoff. 1998. Local adaptation in host-parasite systems. Heredity 81:361–370.

Kaltz, O., S. Gandon, Y. Michalakis, and J. A. Shykoff. 1999. Local maladaptation in the anther-smut fungus *Microbotryum violaceum* to its host plant *Silene latifolia*: evidence from a cross-inoculation experiment. Evolution 53:395–407.

Kawecki, T. J., and D. Ebert. 2004. Conceptual issues in local adaptation. Ecol. Lett. 7:1225–1241.

Kingsolver, J. G., and R. Gomulkiewicz. 2003. Environmental variation and selection on performance curves. Integr. Comp. Biol. 43:470–477.

Lande, R. 1979. Quantitative genetic analysis of multivariate evolution, applied to brain:body size allometry. Evolution 33:402–416.

Lande, R., and S. J. Arnold. 1983. The measurement of selection on correlated characters. Evolution 37:1210–1226.

Lively, C. M., M. F. Dybdahl, J. Jokela, E. E. Osnas, and L. F. Delph. 2004. Host sex and local adaptation by parasites in a snail-trematode interaction. Am. Nat. 164:S6–S18.

McCoy, K. D., T. Boulinier, and C. Tirard. 2005. Comparative host-parasite population structures: disentangling prospecting and dispersal in the black-legged kittiwake Rissa tridactyla. Mol. Ecol. 14:2825–2838.

Morand, S., S. D. Manning, and M. E. J. Woolhouse. 1996. Parasite-host coevolution and geographic patterns of parasite infectivity and host susceptibility. Proc. R. Soc. Lond. B 263:119–128.

Morgan, A. D., S. Gandon, and A. Buckling. 2005. The effect of migration on local adaptation in a coevolving host-parasite system. Nature 437:253–256.

Nagylaki, T. 1980. The strong-migration limit in geographically structured populations. J. Math. Biol. 9:101–114.

Nuismer, S. L. 2006. Parasite local adaptation in a geographic mosaic. Evolution 60:24–30.

Nuismer, S. L., J. N. Thompson, and R. Gomulkiewicz. 1999. Gene flow and

geographically structured coevolution. Proc. R. Soc. Lond. B 266:605–609.

Oppliger, A., R. Vernet, and M. Baez. 1999. Parasite local maladaptation in the Canarian lizard *Gallotia galloti* (Reptilia: Lacertidae) parasitized by haemogregarian blood parasite. J. Evol. Biol. 12:951–955.

Parker, M. A. 1994. Pathogens and sex in plants. Evol. Ecol. 8:560–584.

Prugnolle, F., A. Theron, J. P. Pointier, R. Jabbour-Zahab, P. Jarne, P. Durand, and T. De Meeus. 2005. Dispersal in a parasitic worm and its two hosts: consequence for local adaptation. Evolution 59:296–303.

R Development Core Team. 2006. R: a computing language and environment for statistical computing. R Foundation for Statistical Computing, Vienna.

Soler, J. J., J. G. Martinez, M. Soler, and A. P. Moller. 2001. Coevolutionary interactions in a host-parasite system. Ecol. Lett. 4:470–476.

Thompson, J. N. 1994. The coevolutionary process. The University of Chicago Press, Chicago.

———. 2005. The geographic mosaic of coevolution. University of Chicago Press, Chicago.

Thompson, J. N., S. L. Nuismer, and R. Gomulkiewicz. 2002. Coevolution and maladaptation. Integr. Comp. Biol. 42:381–387.

Thrall, P. H., and J. J. Burdon. 1999. The spatial scale of pathogen dispersal: consequences for disease dynamics and persistence. Evol. Ecol. Res. 1:681–701.

Toju, H., and T. Sota. 2006. Imbalance of predator and prey armament: geographic clines in phenotypic interface and natural selection. Am. Nat. 167:105–117.

Whitlock, M. C., and R. Gomulkiewicz. 2005. Probability of fixation in a heterogeneous environment. Genetics 171:1407–1417.

Zhong, D. B., A. Pai, and G. Y. Yan. 2003. Quantitative trait loci for susceptibility to tapeworm infection in the red flour beetle. Genetics 165:1307–1315.

Associate Editor: R. Mauricio